An Extended Finite Element (XFEM) Approach for Crack Analysis in Composite Media

S.H. Ebrahimi[1], S. Mohammadi[2,*], A. Asadpoure[3]

Abstract. *A new approach is proposed to model a crack in orthotropic composite media using the extended finite element method (XFEM). The XFEM uses the concept of partition of unity in addition to meshless basic idea of approximating a field variable by its values at a set of surrounding nodes. As a result, higher order approximations can be designed with the same total number of degrees of freedom. In this procedure, by using meshless based ideas, elements containing a crack are not required to conform to crack edges. Therefore mesh generating is performed without any consideration of crack conformations for elements and the method has the ability of extending the crack without any remeshing. Furthermore, the type of elements around the crack-tip is the same as other parts of the finite element model and the number of nodes and consequently degrees of freedom are reduced considerably in comparison to the classical finite element method. Developed orthotropic enrichment functions are further modified to enable modeling isotropic problems.*

Keywords: Extended finite element method, orthotropic media, near tip field, crack.

1. Introduction

High strength to weight ratio of composite materials has found wide industrial and engineering applications in recent years. They can be applied in the shape of thin layers while remain very imperfection sensitive. Consequently, their orthotropic fracture behaviour has turned into an interesting active research subject. Some analytical investigation have been reported on the fracture behaviour of composite materials such as the pioneering one by Muskelishvili [1], Sih et al. [2], Tupholme [3], Viola et al. [4], Lim et al. [5] and Nobile and Carloni [6].

Owing to the fact that analytical methods are not considered as feasible methods for solving arbitrary problems, numerical methods such as the boundary element method [7], the finite element method [8], and meshless methods [9]

have been widely expanded and utilized in engineering applications. In many meshless methods, simulation of arbitrary geometries and boundaries is so cumbersome. However, the finite element method is more convenient and applicable because of its ability in modelling general boundary conditions, loadings, materials and geometries. One of its main drawbacks is that elements associated with a crack must conform to crack faces. Furthermore, remeshing techniques are required to follow crack propagation patterns. To improve these drawbacks in modelling discontinuities, Belytschko and Black [10] combined FEM with the partition of unity (proposed by Melenk and Babuška [11], Duarte and Oden [12]), soon to be known as the eXtended Finite Element Method (XFEM). In the XFEM, the finite element approximation is enriched with appropriate functions extracted from the fracture analysis around a crack-tip. The main advantage of the XFEM is its capability in modelling discontinuities independently, so the mesh is prepared without considering the existence of discontinuities. In 2D isotropic media, Mo?s [13] and Dolbow [14] proposed an improvement to the work by Belytschko [10], and Sukumar [15] extended the method to 3D problems. A comprehensive review and discussion on the

---

* *Corresponding author: Email:smoham@ut.ac.ir*

[1] *School of Civil Engineering, University of Tehran, Tehran, Iran*

[2] *School of Civil Engineering, University of Tehran, Tehran, Iran. Email:smoham@ut.ac.ir*

[3] *Department of Civil Engineering, Sharif University of Technology, Tehran, Iran.*

subject can be found in Mohammadi [16].

In the present study, a new set of enrichment functions is derived to simulate orthotropic cracked media using the extended finite element method. Crack-tip enrichment functions used in the extended finite element method are derived from already developed complex functions that determine the stress and displacement fields around a crack-tip. In this paper, first, essential formulations of orthotropic materials are reviewed. Then, the extended finite element method is concisely examined and the crack-tip (near-tip) enrichment functions are obtained. Thereafter, a method used for evaluating stress intensity factors is presented. Finally, in order to examine the robustness and validity of the proposed method, it is used to analyze various numerical examples and to evaluate mixed mode stress intensity factors and to compare them with available results.

2. Orthotropic Media

The strain-stress equation for an orthotropic medium can be defined as

$$\varepsilon = C\sigma \tag{1}$$

where C is the orthotropic compliance matrix. Viola et al. [4] developed a methodology of transformation in order to express the formulation in terms of complex functions. As a result, the set of equations for an in-plane static problem can be expressed as [4]

$$
\begin{Bmatrix}
\dfrac{\partial^2 u_1}{\partial x_1^2} \\
\dfrac{\partial^2 u_1}{\partial x_1 \partial x_2} \\
\dfrac{\partial^2 u_2}{\partial x_1^2} \\
\dfrac{\partial^2 u_2}{\partial x_1 \partial x_2}
\end{Bmatrix}
+ A
\begin{Bmatrix}
\dfrac{\partial^2 u_1}{\partial x_1 \partial x_2} \\
\dfrac{\partial^2 u_1}{\partial x_2^2} \\
\dfrac{\partial^2 u_2}{\partial x_1 \partial x_2} \\
\dfrac{\partial^2 u_2}{\partial x_2^2}
\end{Bmatrix}
=
\begin{Bmatrix}
0 \\ 0 \\ 0 \\ 0
\end{Bmatrix}
\tag{2a}
$$

$$
A = \begin{bmatrix}
0 & \alpha_1 & 2\beta_1 & 0 \\
-1 & 0 & 0 & 0 \\
2\beta_2 & 0 & 0 & \alpha_2 \\
0 & 0 & -1 & 0
\end{bmatrix}
\tag{2b}
$$

Where

$$\alpha_1 = \frac{C_{66}}{C_{11}}, \quad \alpha_2 = \frac{C_{22}}{C_{33}}$$

$$\beta_1 = \frac{C_{12} + C_{33}}{2C_{11}}, \quad \beta_2 = \frac{C_{12} + C_{33}}{2C_{33}} \tag{3}$$

Eigenvalues λ of the matrix $\mathbf{A}$ can be obtained by

$$\lambda^4 + 2b_1\lambda^2 + b_2 = 0 \tag{4}$$

with

$$b_1 = \frac{(\alpha_1 + \alpha_2 - 4\beta_1\beta_2)}{2}, \quad b_2 = \alpha_1\alpha_2 \quad , \tag{5}$$

also defining,

$$\tag{6}$$

$$\gamma_1^2 = \frac{1}{2}\left(\sqrt{b_2} + b_1\right)$$

$$\gamma_2^2 = \frac{1}{2}\left(\sqrt{b_2} - b_1\right) \tag{7}$$

$$l^2 = \left(\gamma_1^2 + \gamma_2^2\right)^{-1} \tag{8}$$

In order to extract the necessary crack tip enrichment functions, near tip displacement fields have to be evaluated for a general traction free crack within an infinite orthotropic plate subjected to uniform biaxial loads at infinity. Figure 1 shows the crack geometry, Cartesian and polar co-ordinates and the loading conditions, consisting of normal stresses and as well as shear load τ.

Neglecting the velocity of the crack propagation for the present static case, the basic solution proposed by Viola et al. [4] results in the following displacement fields in x ad y directions

$$
\begin{aligned}
u_1 = &-2\beta_1\big[(p_3 A_1 - p^4 B_1 + p_4 B_2)Y_1 \\
&+ (p_3 B_1 + p_4 A_1)X_1 + p_3 B_2 X_2\big] \\
&+ \frac{\beta_1 \sigma}{C_{33}A_2}\{(p_3 k_6 + p_4 k_5)[2(a + r\cos\theta) \\
&- \sqrt{2ar}\left(\sqrt{g_1(\theta)}\cos\theta_1/2 + \sqrt{g_2(\theta)}\cos\theta_2/2\right)] \\
&- (p_3 k_5 + p_4 k_5)\sqrt{2ar}\left(\sqrt{g_1(\theta)}\sin\theta_1/2\right. \\
&\left.- \sqrt{g_2(\theta)}\sin\theta_2/2\right)\} + \frac{\beta_1 \tau}{C_{33}A_2}\{(p_3 k_3 + p_4 k_4)[X_1 \\
&- X_2 + \sqrt{2ar}\left(\sqrt{g_2(\theta)}\cos\theta_2/2 - \sqrt{g_1(\theta)}\cos\theta_1/2\right)] \\
&- (p_3 k_4 + p_4 k_3)[2Y_1 - \sqrt{2ar}\left(\sqrt{g_1(\theta)}\sin\theta_1/2\right. \\
&\left.\left(\sqrt{g_2(\theta)}\sin\theta_2/2\right)\right]\}
\end{aligned}
\tag{9}
$$

$$u_2 = -[(\gamma_1 A_1 - \gamma_2 B_1 - \gamma_2 B_2)Y_1$$
$$+ (\gamma_2 A_1 + \gamma_1 B_2)X_1 - \gamma_1 B_2 X_2] + \frac{\sigma}{2C_{33}A_2}\{(\gamma_1 k_6$$
$$+ \gamma_2 k_5)[(X_1 - X_2) + \sqrt{2ar}(\sqrt{g_1(\theta)}\cos\theta_2/2$$
$$- \sqrt{2ar}\cos\theta_2/2] + (\gamma_1 k_5 - \gamma_2 k_6)[2Y_1$$
$$- \sqrt{2ar}(\sqrt{g_1(\theta)}\sin\theta_1/2 + \sqrt{g_2(\theta)}\sin\theta_2/2)]\}$$
$$+ \frac{\tau}{2C_{33}A_2}\{(\gamma_1 k_3 - \gamma_2 k_4)[2(a + r\cos\theta)$$
$$- \sqrt{2ar}(\sqrt{g_1(\theta)}\cos\theta_1/2 + \sqrt{g_2(\theta)}\cos\theta_2/2)]$$
$$+ (\gamma_2 k_3 + \gamma_1 k_4)\sqrt{2ar}(\sqrt{g_1(\theta)}\sin\theta_1/2$$
$$+ \sqrt{g_2(\theta)}\sin\theta_2/2)\} \tag{10}$$

where

$$p_1 + ip_2 = \frac{(\gamma_1 + i\gamma_2)}{\alpha + (\gamma_1 + i\gamma_2)^2} \tag{11}$$

$$p_3 + ip_4 = (\gamma_1 + i\gamma_2)(p_1 - ip_2) \tag{12}$$

and

$$k_1 = \frac{C_{12} - 2\beta_1 p_3 C_{11}}{C_{33}}, \quad k_2 = 2\beta_1 p_4 \frac{C_{11}}{C_{33}}$$
$$k_3 = \frac{C_{22} - 2\beta_1 p_3 C_{12}}{C_{33}}, \quad k_4 = 2\beta_1 p_4 \frac{C_{12}}{C_{33}}$$
$$k_5 = 2\beta_2 p_2 - \gamma_2, \quad k_6 = 2\beta_2 p_1 - \gamma_1 \tag{13}$$

with

$$X_1 = (a + r\cos\theta) - \gamma_1 l^2 r\sin\theta$$
$$X_2 = (a + r\cos\theta) + \gamma_1 l^2 r\sin\theta$$
$$Y_1 = \gamma_2 l^2 r\sin\theta$$
$$A_1 = \frac{(k_3 k - k_1)\sigma}{C_{33}(k_1 k_4 - k_2 k_3)}$$
$$A_2 = k_3 k_6 - k_4 k_5$$
$$B_1 = \frac{\tau}{2C_{33}k_6} + \frac{\sigma}{2C_{33}k_6}\frac{[\kappa(k_4 k_6 - k_3 k_5) + (k_1 k_5 - k_2 k_6)]}{(k_1 k_4 - k_2 k_3)}$$
$$B_2 = -\frac{\tau}{2C_{33}k_6} + \frac{\sigma}{2C_{33}k_6}\frac{[\kappa(k_4 k_6 - k_3 k_5) - (k_1 k_5 + k_2 k_6)]}{(k_1 k_4 - k_2 k_3)} \tag{14}$$

and

$$g_j(\theta) = (\cos^2\theta + l^2\sin^2\theta + (-1)^j l^2\sin2\theta)^{1/2}$$
$$j = 1,2. \tag{15}$$

$$\theta_j = \arctan\left(\frac{\gamma_2 l^2 \sin\theta}{\cos\theta + (-1)^j \gamma_1 l^2 \sin\theta}\right) \tag{16}$$
$$j = 1,2.$$

It is noted that the displacement fields in Eqs. (9-10) are only valid for near crack-tip region: $r/a<1$.

3. Extended Finite Element Method

X-FEM was originally proposed by Belytschko and Black [10] and Dolbow [14] and later modified and applied to various crack analysis problems by Sukumar et al. [15]. A numerical X-FEM model is constructed by dividing the model into two parts; first part is generating a mesh for the domain geometry (neglecting the existence of any crack or other discontinuities) and second part is enriching finite element approximation by appropriate functions for modeling any imperfections.

Consider x is a point of R^2 space in the finite element model and S is a set of nodes defined as $S=\{n_1,n_2,...n_m\}$, m is the number of nodes in the element. The enriched approximation of displacement can be defined by:

$$\mathbf{u}^h(\mathbf{x}) = \overbrace{\sum_{\substack{I \\ n_I \in S}} \phi_I(\mathbf{x})\mathbf{u}_I}^{\text{FEM}} + \overbrace{\sum_{\substack{J \\ n_J \in S_\psi}} \phi_J(\mathbf{x})\psi(\mathbf{x})\mathbf{a}_J}^{\text{enrichment}} \tag{17}$$

where u_I is the classical nodal degree of freedom in FEM, a_J is the added set of degrees of displacement freedom to the standard finite element model, ϕ_I is the shape function associated to node I, $\psi(x)$ is the enrichment function defined over the domain S_ψ:

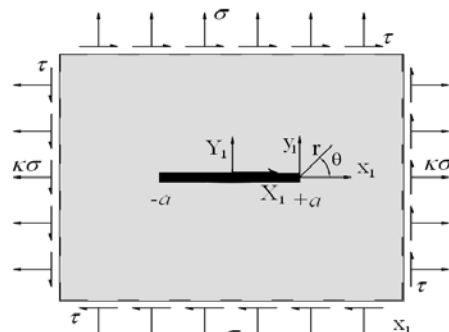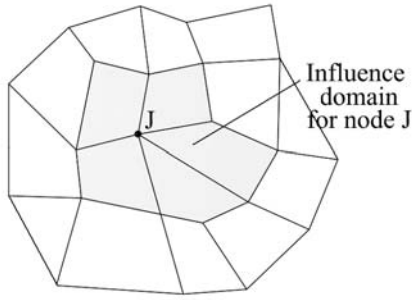**Fig.1** Crack geometry, loading condition and global and local co-ordinates.

200

International Journal of Civil Engineerng. Vol. 6, No. 3, September 2008

Fig.2 Influence (support) domain for node J in an arbitrary finite element mesh

According to the type of discontinuity, $\psi(x)$ can be chosen by applying its associated analytical solutions.

For modeling an arbitrary crack, Eq. (17) can be re-written as [14,16]:

$$\mathbf{u}^h(\mathbf{x}) = \sum_{\substack{I \\ n_I \in S}} N_I(\mathbf{x})\mathbf{u}_I + \sum_{\substack{J \\ n_J \in S_H}} \mathbf{b}_J N_J(\mathbf{x}) H(\mathbf{x})$$

$$+ \sum_{k \in S_1} N_k(\mathbf{x})\left(\sum_l \mathbf{c}_k^{l1} F_l^1(\mathbf{x})\right)$$

$$+ \sum_{k \in S_2} N_k(\mathbf{x})\left(\sum_l \mathbf{c}_k^{l2} F_l^2(\mathbf{x})\right) \qquad (18)$$

where S_1 and S_2 are the domains in which the crack-tip is in its support domain for tip 1 and tip 2, respectively, SH is the domain associated to crack length discontinuity, b_J and c_k^l are vectors of additional nodal degrees of freedom, $F_l^1(x)$ and $F_l^2(x)$ are near-tip branch enrichment functions derived from the two-dimensional asymptotic displacement field near crack-tip and $H(x)$ is the Heaviside function defined as the signed function in this study; the value of +1 if the point is on the positive side of the crack and –1, otherwise:

$$H(\mathbf{x}) = \begin{cases} +1 & \mathbf{x} \in \Omega^+ \\ -1 & \mathbf{x} \in \Omega^- \end{cases} \qquad (19)$$

Nodes that belong to S_1 or S_2 are enriched with the crack-tip enrichment functions $F_1(x)$ and $F_2(x)$ respectively, and those which contain the crack within their support domain and do not belong to S_1 or S_2 are enriched with the Heaviside function $H(x)$.

Crack-tip enrichment functions are obtained from the analytical solutions (9-10) for displacement in the vicinity of a crack-tip: [17]

$$\{F_l(r,\theta)\}_{l=1}^4 = \left\{ \sqrt{r}\cos\frac{\theta_1}{2}\sqrt{g_1(\theta)}, \right.$$

$$\sqrt{r}\cos\frac{\theta_2}{2}\sqrt{g_2(\theta)}, \sqrt{r}\sin\frac{\theta_1}{2}\sqrt{g_1(\theta)},$$

$$\left. \sqrt{r}\sin\frac{\theta_2}{2}\sqrt{g_2(\theta)} \right\} \qquad (20)$$

where θ and $g_j(\theta)$ have been defined in equations (15) and (16).

In Eq. (20), the third and forth functions in the right-hand side of the equation are discontinuous across the crack faces while the others remain continuous.

Developed enrichment functions (20) can be applied for orthotropic materials and can not be directly used for isotropic problems, as they may involve 0/0 or number/0 operations. Mathematical simplifications to remove the ambiguous solutions have been performed to transform (20) into alternative functions for the limiting case of isotropic problems. It is, however, always easier to use the original isotropic near tip enrichment functions.

The discrete system of linear equations in the XFEM in global form can be written as [17]

$$\mathbf{KU} = \mathbf{F} \qquad (21)$$

where $\mathbf{K}$, $\mathbf{U}$ and $\mathbf{F}$ are the stiffness matrix, the vector of degrees of nodal freedom (for both classical and enriched ones) and the vector of external forces, respectively. The global stiffness matrix $\mathbf{K}$ is calculated by an assembly procedure for each element defined as

$$\mathbf{K}_{ij}^e = \begin{vmatrix} \mathbf{k}_{ij}^{uu} & \mathbf{k}_{ij}^{uh} & \mathbf{k}_{ij}^{ut} \\ \mathbf{k}_{ij}^{hu} & \mathbf{k}_{ij}^{hh} & \mathbf{k}_{ij}^{ht} \\ \mathbf{k}_{ij}^{tu} & \mathbf{k}_{ij}^{th} & \mathbf{k}_{ij}^{tt} \end{vmatrix} \qquad (22)$$

where

$$\mathbf{k}_{ij}^{rs} = \int_{\Omega^e} (\mathbf{B}_i^r)^T \mathbf{D} \mathbf{B}_j^s \, d\Omega \quad (r,s = u,h,t) \qquad (23)$$

and $\mathbf{B}$ is the matrix of shape function derivatives,

$$\mathbf{B}_i^u = \begin{bmatrix} N_{i,x} & 0 \\ 0 & N_{i,y} \\ N_{i,y} & N_{i,x} \end{bmatrix} \qquad (24)$$

$$\mathbf{B}_i^h = \begin{bmatrix} (N_i H)_{,x} & 0 \\ 0 & (N_i H)_{,y} \\ (N_i H)_{,y} & (N_i H)_{,x} \end{bmatrix} \tag{25}$$

$$\mathbf{B}_i^t = \begin{bmatrix} \mathbf{B}_i^{t1} & \mathbf{B}_i^{t2} & \mathbf{B}_i^{t3} & \mathbf{B}_i^{t4} \end{bmatrix} \tag{26}$$

$$\mathbf{B}_i^{t\alpha} = \begin{bmatrix} (N_i F_\alpha)_{,x} & 0 \\ 0 & (N_i F_\alpha)_{,y} \\ (N_i F_\alpha)_{,y} & (N_i F_\alpha)_{,x} \end{bmatrix}$$

$$(\alpha = 1,2,3 \text{ and } 4) \tag{27}$$

and the force vector,

$$F_i^e = \left\{ \mathbf{f}_i^u \quad \mathbf{f}_i^h \quad \mathbf{f}_i^{t1} \quad \mathbf{f}_i^{t2} \quad \mathbf{f}_i^{t3} \quad \mathbf{f}_i^{t4} \right\}^{\mathrm{T}} \tag{28}$$

where

$$\mathbf{f}_i^h = \int_{\partial\Omega_r^h \cap \partial\Omega^e} N_i H \bar{\mathbf{t}} \, d\Gamma + \int_{\Omega^e} N_i H \mathbf{b} \, d\Omega \tag{29}$$

$$\mathbf{f}_i^{t\alpha} = \int_{\partial\Omega_r^h \cap \partial\Omega^e} N_i F_\alpha \bar{\mathbf{t}} \, d\Gamma$$

$$+ \int_{\Omega^e} N_i F_\alpha \mathbf{b} \, d\Omega \quad (\alpha = 1,2,3 \text{ and } 4) \tag{30}$$

where Ω^e is an element, Ω^h is an element with a crack lying along its edges, $\partial\Omega$ denotes the boundary of the domain Ω, $\bar{\mathbf{t}}$ is the traction and $\mathbf{b}$ is the body force.

Because the ordinary Gaussian rules do not accurately calculate the integration of enrichment functions in elements cut by a crack, the element has to be subdivided into sub-triangles or sub-quads, as depicted in Figure 3. In this method, a node is enriched if there are Gaussian points at both sides of the crack in the influence domain of the crack. Figure 3b shows a mesh that contains a crack while the second method was applied.
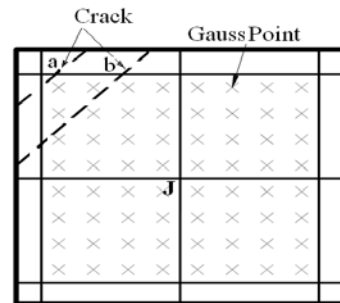
Although the crack "a" cuts the element, node J must not be enriched because there is no Gaussian point above the crack. In contrary, node J has to be enriched for crack "b".

4. Numerical Examples

In this section some examples are presented. For comparing the results, Stress Intensity Factors (SIFs) and J-integral are calculated and
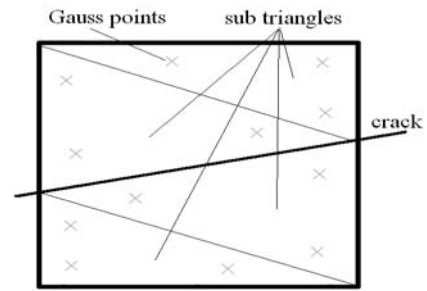
a) gauss integration within sub-triangles

b) gauss integration within sub-quads

Fig.3 Different methods for definition of Gaussian integration points.

compared. These parameters are among the best parameters for determination of the path of crack propagation. In this section, SIFs and J-integral are obtained by the method proposed by Kim and Paulino [18].

4.1. Tensile plate with a central crack

In order to verify the proposed approach, first a classical isotropic rectangular plate with a central crack is considered ($E_{11}=E_{22}$). The infinite tensile plate is discretized by a structured finite element mesh. Different numbers of finite elements (24*50 and 48*90 mesh) are used to assess the accuracy of results.

Figure 5 shows the crack tip and heaviside enrichment nodes. Elements that are fully cut by a crack are enriched by the heaviside enrichment, whereas elements containing a crack tip are enriched by the crack tip enrichment functions (20).

Figure 6 illustrates the J integral contours adopted for the coarse and fine finite element meshes. Element matrices are integrated over the set of Gaussian points as depicted in Figure 7.
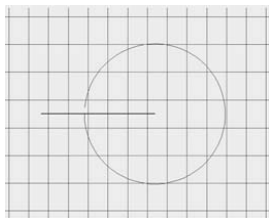
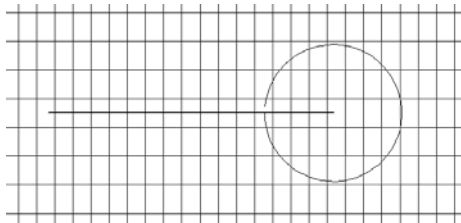Table 1 compares the normalized stress
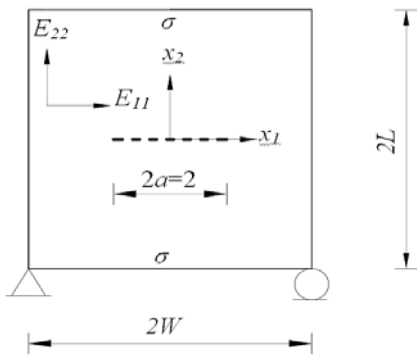
Fig.4 Geometry of the anisotropic tensile plate.
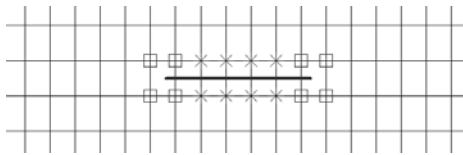
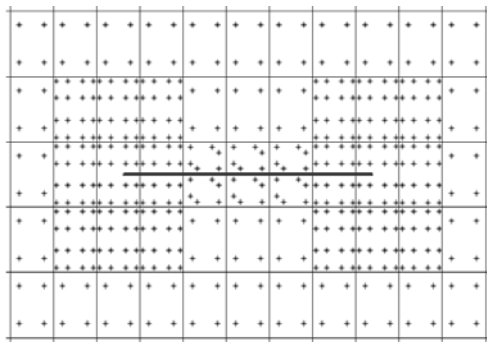**Fig.5** Crack tip (square) and Heaviside (circle) enrichment nodes.

a) 24*50 mesh

b) 48*90 mesh

Fig.6 Contour domains for evaluation of the J integral on each crack tip.


**Fig.7** Contour domains for evaluation of the J integral on each crack tip.

intensity factors for various meshes as well as different ratios of crack length a to plate width w. The computed errors show a close agreement between the numerical results and the exact solution according to the Irwin's classical solution. Figure 8 depicts the distribution of σ_{xx} and σ_{yy} stress components, with a clear indication of concentrated stress field.

In the next stage an orthotropic plate, with a crack aligned along the axis of orthotropy in the center of the plate is studied. At edges parallel to the crack, a constant traction ($\sigma=1$) is applied. Geometry and boundary conditions for the problem are similar to Figure 4.

In the FEM discretization, about 2500 four-node quadrilateral elements are used (Figure 9).

a) σ_{xx} a) σ_{yy}
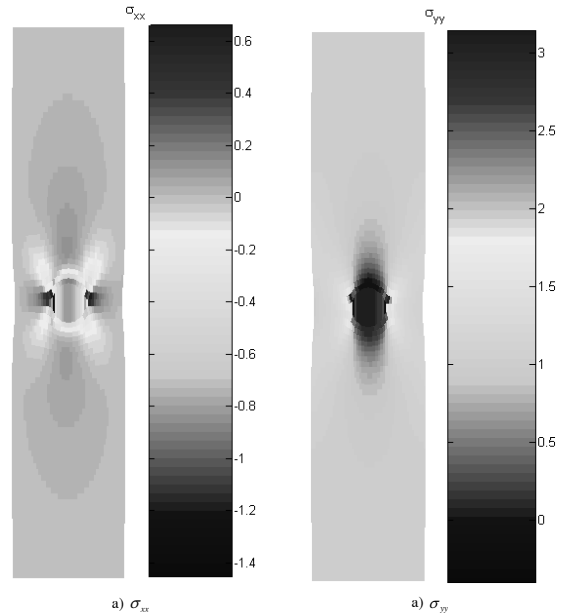
Fig. 8 Stress distribution
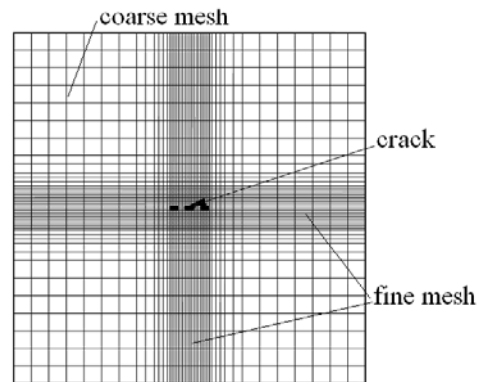
Fig. 9 The discretizated adaptive finite element model.

S.H. Ebrahimi, S.Mohammadi, A.Asadpour

Table 1 Normalized values of stress intensity factors for various discretization and domain

a/w	Irwin	Mesh 24*50		Mesh 48*90	
	$K_I/\sigma\sqrt{\pi a}$	$K_I/\sigma\sqrt{\pi a}$	Error	$K_I/\sigma\sqrt{\pi a}$	Error
1/8.	1.0404	1.0329	-0.72%	1.0346	-0.56%
1/6	1.0746	1.0662	-0.78%	1.0683	-0.59%
1/4	1.1892	1.1796	-0.81%	1.1825	-0.56%

Table 2 Comparison of normalized SIF $\overline{K_I} = K_I/\sigma\sqrt{\pi a}$ with and without crack-tip functions.

contour size (rd/a)	Full enrichment	Without crack-tip function
2	1.019	1.016
0.5	1.018	1.016
0.25	1.019	0.970

Table 3 Comparison of normalized SIF $\overline{K_I} = K_I/\sigma\sqrt{\pi a}$ for the isotropic and orthotropic enrichments.

Φ	Jernkvist [19]		XFEM			
	$\overline{K_I}$	$\overline{K_{II}}$	$\overline{K_I}$	error	$\overline{K_{II}}$	error
0	3.028	0.0	2.960	2.2	0.0	0.0
15	3.033	0.359	3.000	1.1	0.361	0.6
30	3.020	0.685	3.120	3.3	0.691	0.9
45	2.806	0.864	3.029	7.9	0.908	5.1

The size of crack-tip element is one-sixteenth of the crack length, i.e. $h_e/a=1/8$. Stress intensity factors are calculated and compared with those reported by Kim and Paulino [18] ($\overline{K_I} = K_I/\sigma\sqrt{\pi a} = 0.997$), using a total of 2001 elements and 5851 nodes, as shown in Table 2.

Table 2 shows the rate of convergence for various integration domain sizes (r_d) for enrichment with and without crack-tip enrichment functions. As provided in Table 2 small domain sizes can not be used without the inclusion of crack-tip enrichment functions and in order to compensate for the local effects of the crack-tip, larger domains are preferred.

By including crack-tip enrichment functions, higher rates of convergence are anticipated, even for smaller domain sizes around the crack-tip. Numerical results show that when $r_d/a=0.5$, the values of SIFs are independent from the domain size.

Table 3 compares the results for investigating the effect of number of elements in the numerical analysis by utilizing a number of coarse and fine finite elements. In this table, the results for SIFs are compared when isotropic enrichment functions (Dolbow [14]) and the proposed orthotropic method are applied; showing a difference less than half a percent for this particular example.

4.2. A single inclined edge crack specimen

The method proposed in this study is applied to a single edge notched tensile specimen. Geometry of the specimen is shown in Figure 10a and the material properties are defined in Table 4. The finite element mesh of the model consists of 1920 4-noded quadrilateral elements. The model has 14×40 fine elements with 0.075×0.075 cm around the crack and 32×40 elements 0.075×0.15 cm far from the crack (Figure 10b). For the numerical approach, a 2×2 Gauss quadrature is applied for evaluating classical finite element parameters, while for enriched nodes belong to elements that contain a crack, elements are partitioned into 5 sections in both directions and in each section a 6×6 Gauss quadrature rule is utilized.

Mixed mode stress intensity factors have to be

a) Geometry   b) Finite element model
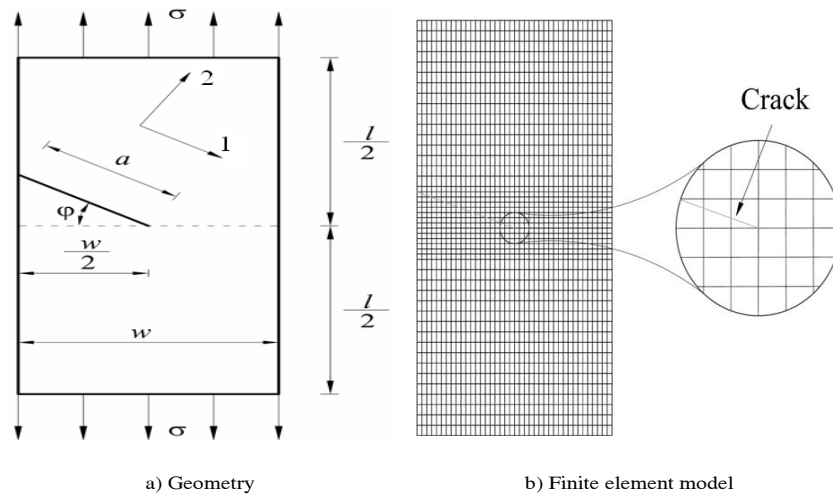
Fig. 10 Specimen geometry of a rectangular plate with single notched cracked.

Table 4 Material properties.

E_1=0.81 GPa	v_{12}=0.56
E_2=0.64 GPa	v_{21}=0.44
G_{12}=0.63 GPa	

Table 5 The effect of crack angle on the normalized stress intensity factor $\overline{K}_i = \frac{K_i}{\sigma\sqrt{\pi a}}$.

Φ	Jernkvist [19]		XFEM			
	$\overline{K}_I$	$\overline{K}_{II}$	$\overline{K}_I$	error	$\overline{K}_{II}$	error
0	3.028	0.0	2.960	2.2	0.0	0.0
15	3.033	0.359	3.000	1.1	0.361	0.6
30	3.020	0.685	3.120	3.3	0.691	0.9
45	2.806	0.864	3.029	7.9	0.908	5.1

evaluated because the crack has an inclination with respect to the line of symmetry. The results are compared in Table 5. The calculated SIFs are based on the converged values corresponding to the case of eight elements far from the crack-tip position. The stress intensity factors reported by Jernkvist [19] were correlated to the load through the usual procedure of identifying displacements of nodal points on the crack surfaces close to the crack-tip by six crack inclinations φ in the range from 0° to 45°.

According to Table 5, while the stress intensity factors are only different within 1-8% for mode I, they are different within 0-5% for mode II. When the crack inclination is low, they are more similar and the maximum differences for the two first inclinations are about 1% and 0.5% for mode I and II, respectively.

Also according to the same table, there is a trend of increasing error as the crack inclination approaches to 45 degrees. It is not a radical change in the level of error, as more or less similar trends are observed in other close angles.

5. Conclusion

In this paper, the problem of modeling cracks in orthotropic media was investigated by the extended finite element approach. The XFEM methodology the finite element model is discretized without any discontinuities. Then the orthotropic asymptotic crack-tip displacement fields as well as Heaviside discontinuous function are added to enrich the finite element approximation using the framework of partition of unity. One of the main advantages is to avoid any explicit meshing of the crack surfaces.

Similarly, no remeshing is required for simulation of crack propagation. The analytical solution for the displacement field is adopted in order to obtain asymptotic crack-tip functions. Mixed-mode stress intensity factors (SIFs) are determined based on the interaction integral approach for evaluation of the J integral. The results are in good agreement with other available numerical or (semi-) analytical methods. In most examples, the maximum difference between the developed method and other available methods has been lass than 2% and 2.5% for modes I and II, respectively. Numerical results have also shown that values of stress intensity factors become independent from the crack tip domain size as it reaches to about a third of the crack length.

6. References

[1]   Muskelishvili NI. Some basic problems on the mathematical theory of elasticity, Noordhoof, Groningen, 1952.

[2]   Sih GC, Paris PC, Irwin GR. On cracks in rectilinearly anisotropic bodies. International Journal of Fracture Mechanics 1 (1965), 189–203.

[3]   Tupholmazqe GE. A study of cracks in orthotropic crystals using dislocations layers. Journal of Engineering and Mathematics 8 (1974), 57–69.

[4]   Viola A, Piva A, Radi E. Crack propagation in an orthotropic medium under general loading. Engineering Fracture Mechanics 34(5) (1989), 1155-1174.

[5]   Lim WK, Choi SY, Sankar BV. Biaxial load effects on crack extension in anisotropic solids, Engineering Fracture Mechanics 68 (2001), 403–416.

[6]   Nobile L, Carloni C. Fracture analysis for orthotropic cracked plates, Composite Structures 68(3) (2005), 285-293.

[7]   Cruse T. Boundary Element Analysis in Computational Fracture Mechanics, Kluwer: Dordrecht, 1988.

[8]   Swenson D, Ingraffea A. Modeling mixed mode dynamic crack propagation using finite elements: Theory and applications. Comput. Mech. 3 (1988) 381-397.

[9]   Belytschko T, Lu YY, Gu L. Element-free Galerkin methods. International Journal for Numerical Methods in Engineering 37 (1994) 229-256.

[10]   Belytschko T, Black T. Elastic crack growth in finite elements with minimal remeshing, Int, J, Num, Meth, Engng. 45 (1999), 601- 620.

[11]   Melenk JM, Babu?ka I. The partition of unity finite element method: basic theory and applications, Computer Methods in Applied Mechanics and Engineering 139 (1996), 289-314

[12]   Duarte CA, Oden JT. An H-p adaptive method using clouds, Computer Methods in Applied Mechanics and Engineering 139 (1996), 237-262.

[13]   Moes N, Dolbow J, Belytschko T, A finite element method for crack growth without remeshing, International Journal for Numerical Methods in Engineering 46 (1999), 131-150.

[14]   Dolbow J, An Extended Finite Element Method with Discontinuous Enrichment for Applied Mechanics, Theoretical and Applied Mechanics, Northwestern University, Evanston, IL, USA: Ph.D. thesis, 1999

[15]   Sukumar N, Mo?s N, Moran B, Belytschko T. Extended finite element method for three-dimensional crack modeling, International Journal for Numerical Methods in Engineering 48 (2000), 1549-1570

[16]   Mohammadi S. Extended Finite Element Method for Fracture Analysis of Structures, Blackwell Publishers, UK (2007).

[17]   Asadpoure A, Mohammadi S, Vafai A. Modeling crack in orthotropic media using a coupled finite element and partition of unity methods. Finite Elements in Analysis and Design (2006) 42/13 pp. 1165-1175.

[18]   Kim JH, Paulino GH. The interaction integral for fracture of orthotropic functionally graded materials: evaluation of stress intensity factors, International Journal of Solids and Structures 40 (2003), 3967-4001

[19]   Jernkvist LO. Fracture of wood under mixed mode loading II Experimental investigation of Picea abies. Engineering Fracture Mechanics 2001; 68:65-57